P6.7 TURBULENT FORM DRAG ON ANISOTROPIC THREE-DIMENSIONAL OROGRAPHY

Andrew Brown *, Nigel Wood and Maria Athanassiadou
Met Office, Bracknell, Berkshire U.K.

1. INTRODUCTION

Allowing for the effects of form drag induced by unresolved small-scale hills in Numerical Weather Prediction models has led to significant improvements in model performance. However, the approach is based on the results of process studies of flow over hills which have almost exclusively concentrated on flow normal to two-dimensional hills, or ridges. The few studies which have considered three-dimensional hills have mainly studied isotropic, circularly symmetric hills. Relatively little attention has been given to the arguably more physically relevant, intermediate case of anisotropic three-dimensional hills. This case may, in an idealized way, be characterized by flow over an ellipsoid with lengths along the horizontal major and minor axes denoted by λ_x and λ_y, respectively. The usual ridge case is then retrieved by letting the aspect ratio $a = \lambda_x/\lambda_y$ go to infinity and the isotropic case has $a = 1$.

Recently Brown and Wood (2001) studied the problem of neutral flow over ellipsoidal hills through a series of numerical simulations in which the aspect ratio and wind direction were varied independently. In this paper we recover their results by using a simple parametrization for the directionally dependent force on a two-dimensional ridge, and summing the contributions from the different Fourier modes which make up the surface topography. We then go on to take the first steps towards extending their results into non-neutral conditions. This is done by examining, through numerical simulations, the variation with wind direction of the force on a ridge in stable conditions.

2. FORM DRAG ON ELLIPSOIDAL HILLS IN NEUTRAL CONDITIONS

The surface configuration used is similar to the "packed" three-dimensional case of Wood and Mason (1993), but here has been generalized so that ellipsoidal as well as axisymmetric hills may be considered. The hill's surface is given by $Z_s(x,y) = h^{3D}\left(\cos\left(\pi\{(x/\lambda_x)^2 + (y/\lambda_y)^2\}^{1/2}\right)\right)^2$ for $(x/\lambda_x)^2 + (y/\lambda_y)^2 \leq 1/4$, and $Z_s(x,y) = 0$ otherwise. Here h^{3D} is the maximum height of the hill, and λ_x and λ_y are the wavelengths in the $x-$ and $y-$ directions respectively. The domain length is set to λ_x and the width to λ_y. Together with the periodic horizontal boundary conditions, this means that we are effectively considering flow over an infinite series hills, closely packed together as indicated in Figure 1. The special case, considered by Wood and Mason (1993), of flow over packed axisymmetric hills is recovered by setting $\lambda_x = \lambda_y$.

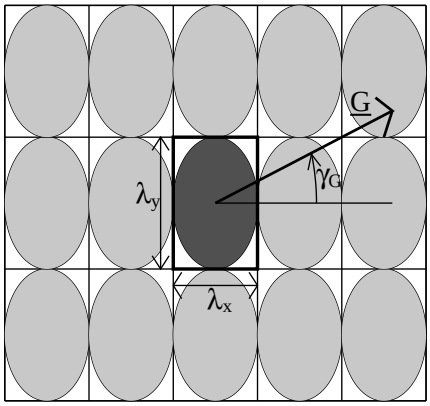

Figure 1: Schematic of the setup. The dark shading indicates the ellipsoidal hill. The boundaries of the domain are indicated with heavy lines. Outside of this domain, the lightly shaded ellipsoids illustrate the periodic images of the hill. The geostrophic wind, G, is at an angle γ_G (positive anticlockwise) from the model $x-$axis. λ_x is the wavelength of the hill in this direction, and λ_y is the wavelength in the normal direction.

Brown and Wood (2001) performed a series of simulations using the BLASIUS model of Wood and Mason (1993). They used a geostrophic wind of 10 ms^{-1} and a surface roughness length of 0.1 m

*Corresponding author address: Andrew Brown, Met Office, Bracknell, Berkshire, RG12 2SZ, U.K.; email: andy.brown@metoffice.com

(resulting in a surface stress, u_*^2, of 0.19 m^{2}s^{-2}), and had $h^{3D} = 50$ m and $\lambda_x = 1000$ m. Six different values of λ_y were used: 1000 m, 1200 m, 1500 m, 2000 m, 3000 m and 6000 m, giving aspect ratios ($a = \lambda_y/\lambda_x$) of 1.0, 1.2, 1.5, 2.0, 3.0 and 6.0. For each of these cases, six different geostrophic wind directions were used: the angle between the geostrophic wind and the model $x-$axis, γ_G, took values of $0°$, $-13°$, $-22.5°$, $-45°$, $-67.5°$ and $-90°$. Additionally, simulations were run with truly two-dimensional ridges (of appropriate height) in order to obtain results from this limiting case.

The calculations presented here exactly parallel these numerical simulations. The pressure force (F_p^{MODE}) on each Fourier mode is aligned normal to the ridge, and the magnitude is predicted using the parametrization of Wood *et al.* (2001):

$$\frac{|F_p^{MODE}|}{S_d} = \alpha\pi^2 u_*^2 \theta^2 \cos^2(\gamma_{\rm G}^{\rm MODE} + \phi) \qquad (1)$$

Here S_d is the surface area of the domain, $\alpha = 12.7$ is a dimensionless constant, θ is the maximum slope of the Fourier mode, γ_G^{MODE} is the angle between the geostrophic wind and the line normal to the ridge, and $\phi = 13°$ is an offset which allows for the wind within the boundary layer being backed relative to the geostrophic wind. The results were obtained by summing over the contributions from all possible Fourier modes, although in practice the drag is dominated by the contributions from just four (single ridges within the domain aligned parallel to the $x-$axis, parallel to the $y-$axis and from the corners to the opposite corners).

Figure 2 shows the magnitude of the predicted pressure force on the hill as a function of aspect ratio and wind direction, and Figure 3 shows the variation of the two components of the force. Here F_{p_g} is the force on the hill in the direction of the geostrophic wind, and F_{p_h} is the force in the normal direction.

For the isotropic hills ($a = 1$), the magnitudes and directions (relative to the geostrophic wind direction) of the pressure force are almost independent of γ_G. This is the expected result, as an isotropic problem should not give results which depend on wind direction. The small differences which do exist are due to changes in the relative positions of the periodic images of the hill as the wind is rotated.

In the other limiting case, that of two-dimensional ridges, both the magnitude and direction (relative to the geostrophic wind) of the pressure drag are sensitive to the wind direction. The largest pressure drags are found when the wind is approximately normal to the ridges. Rotating the wind to be at an angle to

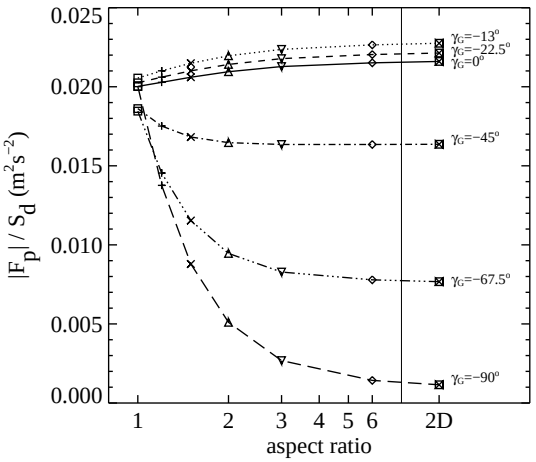

Figure 2: Magnitude of the pressure drag on the three-dimensional hills as a function of aspect ratio, a, and γ_G. The heavy lines link the results with fixed values of γ_G. The light lines link each $a = 6$ result with the appropriate two-dimensional result.

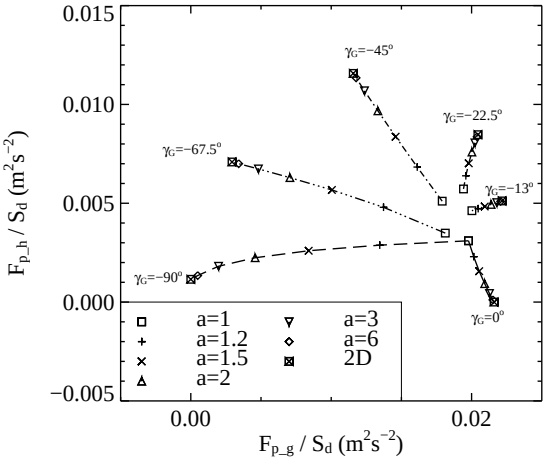

Figure 3: Components of the pressure drag in a coordinate frame aligned with the geostrophic wind.

the ridges results in a reduction of the magnitude of the drag, and also changes its direction (relative to that of the wind) as the pressure drag must remain aligned normal to the ridge. Finally, cases in which the wind is close to parallel to the ridge axes result in very small pressure drags.

The results for flow over anisotropic three-dimensional hills span the range between the limiting cases of flow over isotropic hills (little or no sensitivity to γ_G) and of flow over two-dimensional ridges (strong sensitivity to γ_G). Figures 2 and 3 show that the pressure forces obtained with the most elongated ellipsoidal hills ($a = 6$) are very similar to those obtained in the corresponding two-dimensional simulations. This indicates that three-dimensional effects are not dynamically important in these cases. It is also noteworthy that as the isotropic hills become elongated, the convergence towards these two-dimensional results occurs relatively rapidly. For example, the results obtained with $a = 3$ are already close to those obtained in this limit. Even with a as small as 1.5 the results lie as close to the two-dimensional results as they do to the isotropic ones ($a = 1$). These findings suggest that the two-dimensional limit is a relevant one, and that directional effects are likely to be important even for only moderately anisotropic orography.

Both qualitatively and quantitatively these results are very similar to those obtained by Brown and Wood (2001) in their numerical simulations. This indicates both that the problem is reasonably linear (as expected when considering hills with a maximum slope of 0.03) and that the parametrization (Equation 1) of the force on a two-dimensional ridge is adequate. It also emphasizes that there is nothing mysterious about the rapid convergence of the simulation results of Brown and Wood towards the two-dimensional limit, with the same behaviour being predicted through this consideration of the Fourier decomposition of the surface topography.

3. EXTENSION TO STABLE CONDITIONS

As a first step to extending this work to stable conditions, it was decided to examine the variation with wind direction of the drag on two-dimensional ridges. If it is possible to come up with an accurate prediction of this drag (as done by Equation 1 for neutral conditions), then, as described above, it should be possible to predict the drag on any three-dimensional hill provided that it is within the linear regime.

Numerical simulations have been carried out with the BLASIUS model of Wood and Mason (1993),

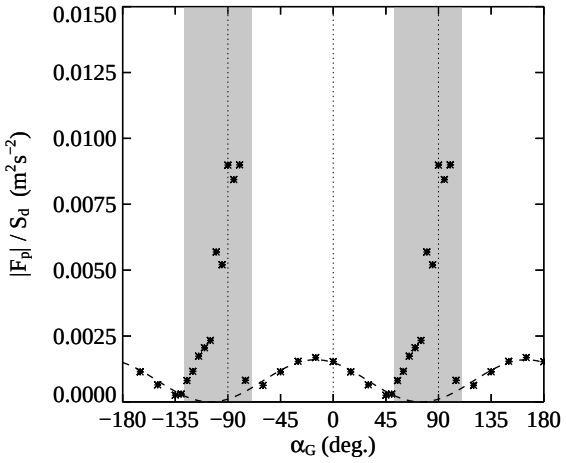

Figure 4: The magnitude of the pressure force as a function of wind direction for the case of stable flow over a ridge described in the text. The symbols show the simulation results. The shaded regions indicate the angles identified as giving wavy solutions. The dashed line shows the predictions of Equation 1 (with $\alpha = 13$).

extended to include stability effects as described in Belcher and Wood (1996). Various different stabilities and ridge wavelengths have been considered, and just one typical example is presented here. This case has a sinusoidal ridge (with roughness length 0.1 m), aligned with the $y-$axis, with peak-to-trough height of 20 m and a wavelength of 2000 m. The geostrophic wind speed is 10 ms^{-1}, and an imposed downward surface buoyancy flux of magnitude 0.0005 m^{2}s^{-3}, leads to the formation of a stable boundary layer approximately 400 m deep, with neutral static-stability aloft. Figure 4 shows the magnitude of the pressure force on the ridge as a function of wind direction. As in the neutral case, there is a maximum in the pressure force when $\alpha_G \simeq -13^\circ$ so that the boundary layer wind is approximately normal to the ridge. For most angles, the variation of the drag with wind direction is also found to be very similar to the cosine-squared dependence obtained in neutral conditions. To illustrate this, the dashed line shows that Equation 1 (with $\alpha = 13.0$) gives a good fit to the simulation results except in the shaded regions. In these regions, the component of the wind normal to the ridge becomes small enough for the boundary layer to admit wave-like solutions. The possibility of obtaining waves within the stable boundary layer was discussed by Chimonas and Nappo (1989), although it is interesting to note that it has been achieved

here even with neutral stability above the boundary layer. The simulations indicate that the details of the flow response in these wavy cases are sensitive to the presence or otherwise of critical lines (consistent with the arguments of Nappo and Chimonas (1993)). Here it is simply noted that the resulting surface pressure forces are typically larger than those obtained in the cases without waves, and in several cases are large compared even to that obtained with flow normal to the ridge.

4. CONCLUSIONS

The turbulent form drag on ellipsoidal hills in neutral conditions has been found to be strongly dependent on wind direction even with only moderate levels of anisotropy. This suggests that directional-dependence might usefully be incorporated in numerical weather prediction model parametrizations, which currently typically predict a drag which is independent of wind direction.

For flow over low hills in stable conditions, the variation of the turbulent form drag with wind direction is found to be similar to that obtained in neutral conditions. However, it has also been found that rotating the wind to become more parallel to a ridge may result in the cross-ridge component of the wind becoming sufficiently small for the stable boundary layer to admit wave-like solutions which lead to increased drag.

5. REFERENCES

Belcher, S. E. and Wood, N., 1996: Form and wave drag due to stably stratified turbulent flow over low ridges. *Quart. J. Roy. Meteorol. Soc.*, **122**, 863–902.

Brown, A. R. and Wood, N., 2001: Turbulent form drag on anisotropic three-dimensional orography. *Boundary-Layer Meteorol.*, **101**, 229–241.

Chimonas, G. and Nappo, C. J., 1989: Wave drag in the planetary boundary layer over complex terrain. *Boundary-Layer Meteorol.*, **47**, 217–232.

Nappo, C. J. and Chimonas, G., 1992: Wave exchange between the ground surface and a boundary-layer critical level. *J. Atmos. Sci.*, **49**, 1075–1091.

Wood, N., Brown, A. R. and Hewer, F. E., 2001: Parametrizing the effects of orography on the boundary layer: An alternative to effective roughness lengths. *Quart. J. Roy. Meteorol. Soc.*, **127**, 759–777.

Wood, N. and Mason, P. J., 1993: The pressure force induced by neutral, turbulent flow over hills. *Quart. J. Roy. Meteorol. Soc.*, **119**, 1233–1267.